Kinetic Mechanism of Human Glutathione-Dependent Formaldehyde Dehydrogenase†

Paresh C. Sanghani,‡ Carol L. Stone,§ Bruce D. Ray,|| Evgenia V. Pindel,‡ Thomas D. Hurley,‡ and William F. Bosron*,‡

Department of Biochemistry and Molecular Biology, Indiana University School of Medicine, Indianapolis, Indiana 46202-5122, Department of Physics, Indiana University-Purdue University at Indianapolis, Indianapolis, Indiana 46202, and Department of Chemistry and Chemical Biology, Stevens Institute of Technology, Hoboken, New Jersey 07030

Received December 28, 1999; Revised Manuscript Received June 27, 2000

ABSTRACT: Formaldehyde, a major industrial chemical, is classified as a carcinogen because of its high reactivity with DNA. It is inactivated by oxidative metabolism to formate in humans by glutathione-dependent formaldehyde dehydrogenase. This NAD^+-dependent enzyme belongs to the family of zinc-dependent alcohol dehydrogenases with 40 kDa subunits and is also called ADH3 or χ-ADH. The first step in the reaction involves the nonenzymatic formation of the *S*-(hydroxymethyl)glutathione adduct from formaldehyde and glutathione. When formaldehyde concentrations exceed that of glutathione, nonoxidizable adducts can be formed in vitro. The *S*-(hydroxymethyl)glutathione adduct will be predominant in vivo, since circulating glutathione concentrations are reported to be 50 times that of formaldehyde in humans. Initial velocity, product inhibition, dead-end inhibition, and equilibrium binding studies indicate that the catalytic mechanism for oxidation of *S*-(hydroxymethyl)glutathione and 12-hydroxydodecanoic acid (12-HDDA) with NAD^+ is random bi-bi. Formation of an E·NADH·12-HDDA abortive complex was evident from equilibrium binding studies, but no substrate inhibition was seen with 12-HDDA. 12-Oxododecanoic acid (12-ODDA) exhibited substrate inhibition, which is consistent with a preferred pathway for substrate addition in the reductive reaction and formation of an abortive E·NAD^+·12-ODDA complex. The random mechanism is consistent with the published three-dimensional structure of the formaldehyde dehydrogenase·NAD^+ complex, which exhibits a unique semi-open coenzyme−catalytic domain conformation where substrates can bind or dissociate in any order.

Human glutathione-dependent formaldehyde dehydrogenase or the class III alcohol dehydrogenase (ADH3)[1,2] is an important component of cellular metabolism for the elimination of formaldehyde from environmental and endogenous sources. Formaldehyde is a potent irritant and sensitizing agent that causes lacrymation, rhinitis, pharyngitis, and contact dermatitis because of its reactivity (*2*). Formaldehyde also induces tumors in nasal epithelium of rats (*2*−*4*). It is classified as a group 2A carcinogen on the basis of animal and human studies (*5*). The cellular strategy for dealing with formaldehyde is to initially oxidize it to the less reactive formate, which is either oxidized to carbon dioxide or incorporated via normal metabolic pathways into the one-carbon pool of the body (*6*).

Human glutathione-dependent formaldehyde dehydrogenase (hereafter called formaldehyde dehydrogenase, FDH) plays an important role in formaldehyde detoxification by catalyzing the oxidation of its adduct *S*-(hydroxymethyl)-glutathione (a spontaneous adduct formed between glutathione and formaldehyde, Figure 1A, **I**) to *S*-formylglutathione with concomitant reduction of a molecule of NAD^+ to NADH. *S*-Formylglutathione is then hydrolyzed to glutathione and formic acid by a hydrolase (*7*).

As an alcohol dehydrogenase, formaldehyde dehydrogenase shares many properties with members of the medium-chain, zinc-containing alcohol dehydrogenase family (*8*), which has been divided into seven distinct enzyme classes based upon sequence homology, catalytic properties, and patterns of gene expression (*1*). Formaldehyde dehydrogenase belongs to class III (ADH3). Like other alcohol dehydrogenases, formaldehyde dehydrogenase is composed of two identical 40 kDa subunits forming a homodimer that contains 4 mol of zinc per dimer. It prefers long-chain alcohols such as ω-hydroxy fatty acids as substrates versus short-chain alcohols such as ethanol (*9*). The Michaelis−Menten constant, K_m, of formaldehyde dehydrogenase for ethanol is greater than 2 M (*10*).

† This work was supported by Grants T32-AA07462, R37-AA07117, and R21-AA11635 from the National Institutes of Health.

* To whom correspondence should be addressed: Department of Biochemistry and Molecular Biology, Indiana University School of Medicine, Room 4023, 635 Barnhill Dr., Indianapolis, IN 46202-5122. E-mail: wbosron@iupui.edu. Phone: (317) 274-7211. Fax: (317) 274-4686.

‡ Indiana University School of Medicine.

§ Stevens Institute of Technology.

|| Indiana University-Purdue University at Indianapolis.

[1] According to a recent classification, the gene encoding class III alcohol dehydrogenase (χ-ADH) or the glutathione-dependent formaldehyde dehydrogenase is called ADH3 (*1*).

[2] Abbreviations: FDH, formaldehyde dehydrogenase; 12-HDDA, 12-hydroxydodecanoic acid; 12-ODDA, 12-oxododecanoic acid; 12-ADDA, 12-aminododecanoic acid; HMGSH, *S*-(hydroxymethyl)-glutathione; IPTG, isopropyl β-D-thiogalactopyranoside; ADH, alcohol dehydrogenase; [^{13}C]HCHO, ^{13}C-labeled formaldehyde.

10.1021/bi9929711 CCC: $19.00
Published on Web 08/08/2000

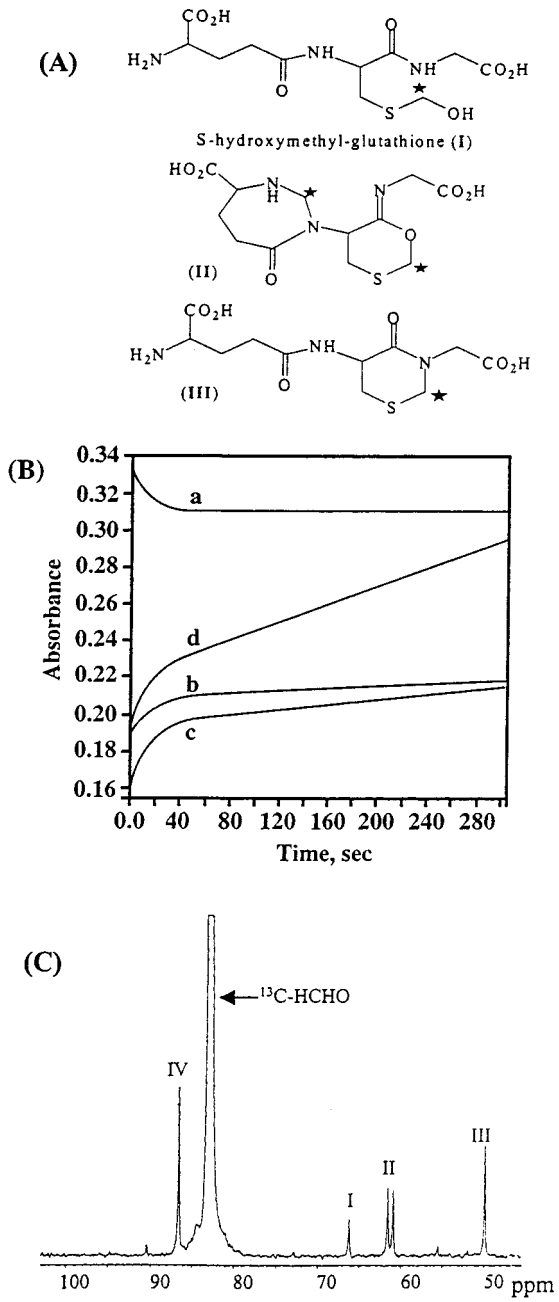

FIGURE 1: Adducts of glutathione and formaldehyde. (A) Structures of the major adducts formed in a mixture of glutathione and formaldehyde as reported previously (*22*). The marked carbon (*) originates from formaldehyde. (B) Absorbance of a mixture of glutathione and formaldehyde. The initial 2 mM glutathione solution in 0.1 M phosphate buffer (pH 7.5) had an absorbance of 0.338. Variable amounts of formaldehyde were added (traces a−d correspond to 1, 6, 15, and 60 mM formaldehyde, respectively) and the absorbance of the mixture observed at 240 nm. (C) ^{13}C NMR of a mixture of 2 mM glutathione and 50 mM [^{13}C]HCHO. Peak I corresponds to *S*-(hydroxymethyl)glutathione. Peaks II and III correspond to compounds **II** and **III** in panel A, respectively. The structure of the compound at 88 ppm was not identified.

The importance of formaldehyde dehydrogenase activity for the cell is evident from the fact that it is highly conserved throughout evolution and is expressed in all mammalian tissues studied so far (*11*). Phylogenetic analysis suggests that formaldehyde dehydrogenase is the evolutionarily oldest form of alcohol dehydrogenase (*12*, *13*). Biochemical and immunocytochemical studies have shown that the cytosolic formaldehyde dehydrogenase is also localized over condensed chromatin, leading to the suggestion that it may protect DNA from formaldehyde modification (*14*).

Reports of the kinetic mechanism of human liver formaldehyde dehydrogenase have been conflicting. The kinetic mechanism was found to be sequential random bi-bi for *S*-(hydroxymethyl)glutathione oxidation (*15*, *16*) but ordered for octanol (*10*). Furthermore, an allosteric regulatory site was proposed for glutathione in addition to binding sites for *S*-(hydroxymethyl)glutathione (*16*). In this study, we report the characterization of adducts formed with formaldehyde and glutathione and the identification of the reaction mechanism of formaldehyde dehydrogenase for oxidation of *S*-(hydroxymethyl)glutathione and 12-HDDA determined by steady-state kinetic analysis and equilibrium binding studies.

MATERIALS AND METHODS

All chemicals were obtained from Sigma-Aldrich.

Expression and Purification of Recombinant Formaldehyde Dehydrogenase. The χ-ADH cDNA clone was obtained from Goldman et al. (*17*). Using a PCR-based method, three changes were made in the open reading frame (deletion of the N-terminal sequence of Met1−Asn18; substitution of Asp and Phe for Tyr185 and Leu264, respectively) to obtain a sequence that matched the χ-ADH cDNA sequence reported by Sharma et al. (*18*). The cDNA was subcloned into the pKK223-3 expression vector (Pharmacia Biotech Inc.) and the correct sequence verified by dideoxynucleotide sequencing. For expression, a starter culture of 50 mL of TB broth containing 50 μg/mL ampicillin was inoculated with 1 mL of a frozen *Escherichia coli* TG-1 cell stock that had been transformed with the expression vector. After about 3 h, this culture was used to inoculate a 20 L culture of TB broth containing 12 g of yeast extract, 12 g of peptone, and 4 mL of glycerol per liter, with 17 mM KH_2PO_4, 72 mM K_2HPO_4, and 50 μg/mL ampicillin. When A_{595} was equal to 0.6−0.8, 0.1 mM isopropyl β-D-thiogalactopyranoside (IPTG) was added to induce expression. Following the addition of IPTG, the cells were grown for an additional 8−10 h at 15 °C before harvesting with a concentrator (Millipore Pellicon) equipped with a 0.45 μm filter. The concentrated cells were centrifuged at 4500*g* for 20 min, and the cells were lysed in a bead beater (Bio-Spec, Bartlesville, OK) in 10 mM Tris buffer (pH 8.0) containing 1 mM benzamidine, 10 μM zinc sulfate, and 2 mM DTT (lysate buffer). The purification of FDH from the cell lysate was similar to that described for $\beta_1\beta_1$ ADH from *E. coli* (*19*). Briefly, the lysate was centrifuged at 100000*g* for 30 min. The supernatant was added to DE52 ion-exchange resin (Whatman Inc.), preequilibrated with the lysate buffer. The unbound protein was collected, and the buffer was exchanged with fresh lysate buffer by ultrafiltration (Millipore Minitan, Bedford, MA) until the conductivity of the enzyme solution was identical with that of the lysate buffer. The enzyme was then loaded onto a Mimetic Blue-2 affinity column (Promimetic Biosciences Inc., Burtonsville, MD) equilibrated with the lysate buffer, and enzyme-containing fractions were eluted with a 0 to 10 mM NAD^+ gradient. Active fractions were directly loaded onto a Q-Sepharose column (Sigma-Aldrich) equilibrated with the lysate buffer, and the enzyme was eluted with a 0 to 0.5 M NaCl gradient. The fractions were analyzed by SDS−PAGE, and the purified enzyme (>90%) was concentrated using an

Amicon Centriprep concentrator to a concentration of 20 mg/mL. The enzyme was stored at −20 °C in 50% glycerol. Yields were about 140 mg of purified protein per 20 L of *E. coli* culture.

The enzyme activity was assayed spectrophotometrically at 25 °C in 100 mM glycine buffer (pH 10) containing 4.7 mM cinnamyl alcohol and 2.5 mM NAD^+ by using a Lambda 6 spectrophotometer (Perkin-Elmer). Enzyme activity units were expressed as micromoles of NADH produced per minute using an absorbance of NADH of 6.22 mM^{-1} cm^{-1} at 340 nm. The purified enzyme after Q-Sepharose chromatography had a specific activity of 5.1 units/mg. Protein concentrations were determined by the Bio-Rad protein assay using bovine serum albumin as the standard.

Analysis of the Glutathione and Formaldehyde Reaction Using ^{13}C NMR and UV Spectrophotometry. Spectrophotometric measurements were performed at 240 nm on a Perkin-Elmer Lambda 6 spectrophotometer. Adduct formation was initiated by mixing the glutathione and formaldehyde stock solutions in 100 mM potassium phosphate (pH 7.5) at 25 °C. The change in absorbance at 240 nm following the initiation of the reaction was monitored with time.

^{13}C NMR was used to analyze the structure of adducts formed when glutathione and [^{13}C]HCHO were mixed under the conditions used in the spectrophotometric analysis. ^{13}C NMR measurements were taken at 75.4 MHz on a Varian UNITY-300 NMR spectrometer equipped with a high-stability variable-temperature controller and 10 mm broadband probe. All sample volumes were 2.5 mL. Samples were buffered with 100 mM potassium phosphate (pH 7.5) and included 0.8 mL of ^2H_2O for field-frequency locking. Spectral parameters were as follows: sweep width, 5280 Hz; number of data points, 8192; recycle delay, 6.3 s; number of transients, 256; ^1H decoupling, frequency modulated during acquisition only; and pulse width, 60°. Processed spectra were zero-filled to 16 384 data points and Fourier transformed with 5 Hz line broadening. The temperature was maintained at 25 °C during the NMR experiment.

Determination of the Equilibrium Constant for Formation of S-(Hydroxymethyl)glutathione Using Stopped-Flow Kinetics. Stopped-flow kinetics were assessed at 25 °C using an Applied Photophysics SX-18MV instrument. These experiments were initiated by mixing varying concentrations of glutathione (0.75−5 mM) with formaldehyde (0.5 mM) in 0.1 M phosphate buffer (pH 7.5). The formation of *S*-(hydroxymethyl)glutathione was monitored spectrophotometrically at 240 nm. Exponential traces were analyzed by nonlinear regression analysis using the Applied Photophysics software. The data were fit to the single-exponential equation (eq 1):

$$A = A_o e^{-kt} + C \quad (1)$$

where A is the absorbance of the mixture at 240 nm, A_o is the amplitude, and k, t, and C are the observed rate constant, time, and constant, respectively. The amplitude was plotted against the final glutathione concentration to obtain the change when all of the formaldehyde had been converted to *S*-(hydroxymethyl)glutathione. This allowed us to calculate the amount of *S*-(hydroxymethyl)glutathione formed at each glutathione concentration. The K_{eq} was calculated using eq 2:

$$K_{eq} = \frac{[HMGSH]}{([GSH]_t - [HMGSH])([HCHO]_t - [HMGSH])} \quad (2)$$

where $[GSH]_t$ and $[HCHO]_t$ are the calculated concentrations of glutathione and formaldehyde in the observation window, respectively, and [HMGSH] is the calculated concentration of *S*-(hydroxymethyl)glutathione from the amplitudes of the reaction.

Synthesis of 12-ODDA. 12-ODDA was prepared by oxidizing 12-HDDA using pyridinium dichromate according to the method of Corey and Schmidt (*20*) with minor modifications. Briefly, 1.4 g of 12-HDDA was dissolved in 750 mL of dried dichloromethane by stirring and warming at 35 °C in a round-bottomed flask. After the mixture was allowed to cool to 25 °C, 12 g of pyridinium dichromate was added with brisk stirring. After 15 min, the mixture was evaporated at reduced pressure at room temperature. Fifty milliliters of a 60:40 mixture of dichloromethane and acetonitrile was added to the residue, and the mixture was loaded onto a silica column equilibrated with the same solvent mixture. The column was eluted with the same mixture, and fractions were collected. 12-ODDA was the first compound to elute from the column, and the fractions were pale yellow. Fractions were analyzed by TLC with an 80:20 dichloromethane/acetonitrile mixture as the development solvent. Compounds were identified on TLC plates with 0.04% bromocresol spray (*21*). Fractions containing 12-ODDA were combined, and the dichloromethane in the solvent mixture was evaporated. 12-ODDA in the acetonitrile mixture was diluted 10-fold with water, and the solvent was removed by freeze-drying. The purified pale white compound was analyzed by TLC and electrospray ionization mass spectrometry (Finnigan LCQ instrument). Mass spectrometric analysis showed an ion at m/z 213.7 [$(M - H)^-$]. The compound was found to be greater than 90% pure and devoid of the starting material 12-HDDA.

Kinetic Methods. Enzyme activity was assayed by monitoring the production or depletion of NADH at 340 nm while studying the reaction in the forward [oxidation of *S*-(hydroxymethyl)glutathione or 12-HDDA] or reverse (reduction of 12-ODDA) direction, respectively. Enzyme activity units are expressed as micromoles of NADH produced or utilized per minute at 340 nm. *S*-(Hydroxymethyl)glutathione studies were performed in 100 mM potassium phosphate (pH 7.5) at 25 °C in cuvettes with a path length of 10 cm. The initial concentrations of glutathione and formaldehyde to be mixed for a desired *S*-(hydroxymethyl)glutathione were calculated using eq 2 with a K_{eq} of 1.77 mM^{-1}. In all the experiments, the ratio of initial glutathione concentration to that of formaldehyde varied from 2 to 800. During each assay, glutathione and formaldehyde were allowed to equilibrate for 2 min in 100 mM potassium phosphate (pH 7.5) at 25 °C before addition of the remaining components to initiate the assay. Studies involving 12-HDDA or 12-ODDA were performed under the same conditions [100 mM potassium phosphate (pH 7.5) at 25 °C], with cuvettes with a path length of 5 or 10 cm.

All studies were performed on a Perkin-Elmer Lambda 6 UV−visible spectrophotometer. Estimates of the initial rates were obtained from linear regression of absorbancies with durations from 15 s to 5 min. Less than 15% of the substrate was consumed over the reaction time course.

Data Analysis. The initial velocity data were fit to either the Michaelis−Menten mechanism (eq 3) or the two-substrate sequential mechanism (eq 4).

$$v = \frac{V_{max}[A]}{[A] + K_m} \quad (3)$$

$$v = \frac{V_{max}[A][B]}{K_{ia}K_b + K_b[A] + K_a[B] + [A][B]} \quad (4)$$

The data from dead-end and product inhibition studies were fit to one of the linear inhibition equations for competitive inhibition (eq 5), noncompetitive inhibition (eq 6), or uncompetitive inhibition (eq 7).

$$v = \frac{V_{max}[A]}{K_m(1 + [I]/K_{is}) + [A]} \quad (5)$$

$$v = \frac{V_{max}[A]}{K_m(1 + [I]/K_{is}) + [A](1 + [I]/K_{ii})} \quad (6)$$

$$v = \frac{V_{max}[A]}{K_m + [A](1 + [I]/K_{ii})} \quad (7)$$

In eqs 3−7, [A], [B], and [I] represent the concentrations of substrates A and B and inhibitor I, respectively. K_m and V_{max} are the Michaelis−Menten constant and maximal velocity, respectively. In eq 4, K_a and K_b represent the Michaelis constants of substrates A and B, respectively. K_{ia} represents the dissociation constant of A for dissociation from the E·A binary complex. For a rapid equilibrium random mechanism, eq 4 is symmetrical for both substrates. Hence, when B is the varied substrate and A is the fixed varied substrate, the constant K_{ia} would now represent the dissociation constant of B. K_{ii} and K_{is} in eqs 5−7 are the dissociation constants of a dead-end inhibitor from the E·A·I ternary complex and E·I binary complex, respectively. However, when eqs 5−7 were used to fit the data from the product inhibition experiment, K_{ii} and K_{is} are apparent inhibition constants of the product inhibitor. Curve fitting was performed by nonlinear regression analysis (GRAFIT, version 4.0.10).

Equilibrium Binding Studies. The binding of NAD^+ and 12-ODDA to the enzyme was examined by measuring the induced changes in intrinsic tryptophan fluorescence of FDH upon binding. The changes in intrinsic tryptophan fluorescence were measured at an excitation wavelength of 300 nm and an emission wavelength of 340 nm. All studies were conducted in 50 mM phosphate buffer (pH 7.5) at 25 °C and using a Fluoromax-2 fluorescence spectrometer (Instruments S.A., Inc., Edison, NJ). The NAD^+ binding studies were conducted by adding coenzyme in small increments to a 5 μM enzyme solution in a volume of 1 mL. There was no significant inner filter effect at the maximal NAD^+ concentration of 190 μM used in the studies. Binding studies with 12-ODDA were conducted in a volume of 3 mL employing enzyme concentrations of 0.1−0.2 μM.

The extent of binding of NADH to the free enzyme was determined by excitation of tryptophan at 290 nm and monitoring the emission of NADH at 460 nm after resonance energy transfer from tryptophan to NADH. The NADH binding studies were conducted using 0.1−0.2 μM enzyme in a volume of 3 mL.

Binding of 12-HDDA to the E·NADH complex was monitored by measuring the enhancement in resonance energy transfer of FDH-bound NADH after addition of 12-HDDA. In these studies, 1 μM enzyme was preequilibrated with 5 μM NADH to ensure that >99% of the enzyme was in the E·NADH complex. 12-HDDA was added in increments, and the enhancement in resonance energy transfer was assessed by exciting at 290 nm and monitoring the emission at 460 nm.

For determination of dissociation constants, the maximal change in fluorescence when all of the enzyme was bound by ligand was calculated initially by fitting the observed changes in fluorescence at a given ligand concentration to the Michaelis−Menten equation. The concentrations of the bound and free ligand were calculated at each total ligand concentration. The data were then analyzed by the Scatchard equation to determine the number of binding sites and the dissociation constant of the ligand.

RESULTS

Identification of the Conditions for the Formation of S-(Hydroxymethyl)glutathione Using ^{13}C NMR and UV Spectrophotometry. Glutathione and formaldehyde yield different adducts depending on the pH and initial concentrations of glutathione and formaldehyde. Several of these adducts that exist in equilibrium have been identified (Figure 1A) (*22*). The rate and conditions under which these adducts form have not been characterized because of the reversibility of their formation and the difficulty of their detection. Previous studies of the kinetic mechanism of glutathione-dependent formaldehyde dehydrogenase using *S*-(hydroxymethyl)glutathione as the substrate have not identified the adducts formed in the assay (*15*, *16*). Appearance of adducts without a free primary hydroxyl group that can be oxidized would either decrease the *S*-(hydroxymethyl)glutathione available or act as inhibitors for the enzyme reaction.

The ionized sulfydryl group of glutathione absorbs at 240 nm. This property has been used to estimate the dissociation constant for *S*-(hydroxymethyl)glutathione formation (*16*). The level of absorption of glutathione decreased initially after addition of formaldehyde as previously reported (Figure 1B, trace a) (*16*). The change in the absorption of the mixture was influenced by the initial glutathione and formaldehyde concentrations that were used. When the initial concentrations of glutathione were equal to or greater than that of formaldehyde, the level of absorption of the mixture rapidly decreased and remained constant for several minutes (Figure 1B, trace a). The rate and extent of decrease in the absorption was found to be proportional to the difference between the initial concentrations of glutathione and formaldehyde. However, when the initial concentrations of formaldehyde were higher than those of glutathione, the initial rapid decrease in the level of absorption was followed by a slower increase in the level of absorption over a period of minutes (Figure 1B, traces b−d). The rate and extent of the initial decrease in absorption followed by its increase were dependent on the excess of formaldehyde over glutathione.

^{13}C NMR was used to identify the adducts formed when glutathione and formaldehyde were mixed. Under conditions in which the initial concentration of glutathione was equal

to or greater than that of [^{13}C]HCHO (conditions showing absorption changes similar to that shown in trace a of Figure 1B), only peaks corresponding to free [^{13}C]HCHO and *S*-(hydroxymethyl)glutathione were observed, suggesting that *S*-(hydroxymethyl)glutathione was the predominant adduct. However, under conditions in which the initial [^{13}C]HCHO concentration was greater than that of glutathione (conditions similar to that in trace d of Figure 1B), formation of two additional adducts was evident by appearances of new peaks in the NMR spectrum of the mixture (Figure 1C, peaks II−IV). Peaks I−III could be assigned to compounds **I**−**III** shown in Figure 1A on the basis of the previously reported chemical shifts (*22*). Thus, ^{13}C NMR and UV spectrophometric analysis showed that *S*-(hydroxymethyl)glutathione is the predominant (perhaps the only) adduct of glutathione and formaldehyde in 100 mM phosphate buffer (pH 7.5) during the time of the kinetic assays (~7 min), when the initial concentrations of glutathione were equal to or greater than that of formaldehyde.

Determination of the Equilibrium Constant for S-(Hydroxymethyl)glutathione Formation. The equilibrium constant for the formation of the *S*-(hydroxymethyl)glutathione adduct from glutathione and formaldehyde was determined using a stopped-flow apparatus to monitor the change in absorbance of the mixture at 240 nm with time. Glutathione was maintained at concentrations equal to or greater than that of formaldehyde throughout the course of the experiment. The changes in the level of absorption of the mixture followed single-exponential kinetics (similar to curve a of Figure 1B). The amplitude was proportional to the amount of *S*-(hydroxymethyl)glutathione adduct formed. The K_{eq} value, calculated from eq 2, was found to be 1.77 ± 0.13 mM.

Initial Velocity, Product Inhibition, and Dead-End Inhibition Studies of the Oxidation of S-(Hydroxymethyl)glutathione and 12-HDDA. The kinetic mechanism was elucidated for both *S*-(hydroxymethyl)glutathione and 12-HDDA. While the hydroxyl group in 12-HDDA is a typical primary alcohol group whose oxidation by alcohol dehydrogenases has been widely studied, the hydroxyl group in *S*-(hydroxymethyl)-glutathione is attached to a carbon which is adjacent to an electron-rich sulfur, which could facilitate the transfer of hydride to the cofactor NAD^+. The instability of *S*-formylglutathione (*15*) prevented the study of the reverse reaction, but 12-ODDA was synthesized chemically by a one-step oxidation of 12-HDDA and utilized for aldehyde reduction kinetics.

The alcohol oxidation reaction was studied by varying the substrate concentrations [*S*-(hydroxymethyl)glutathione or 12-HDDA] at different fixed NAD^+ concentrations. An example of a double-reciprocal plot is shown in Figure 2. In contrast to previously reported nonlinear plots (*16*), the double-reciprocal plots for *S*-(hydroxymethyl)glutathione and 12-HDDA were linear and intersected on the left of the ordinate, which is consistent with a sequential kinetic mechanism. The data for both the substrates fit well to the sequential bireactant mechanism (eq 4). Kinetic constant values obtained from the nonlinear regression are shown in Table 1. The catalytic efficiency (k_{cat}/K_a) of *S*-(hydroxymethyl)glutathione oxidation is about 125-fold higher than that of 12-HDDA at pH 7.5. The double-reciprocal plots of 12-HDDA at fixed varying NAD^+ levels at pH 10 were also linear (data not shown). The k_{cat} for 12-HDDA oxidation was 26-fold higher at pH 10 than at pH 7.5.

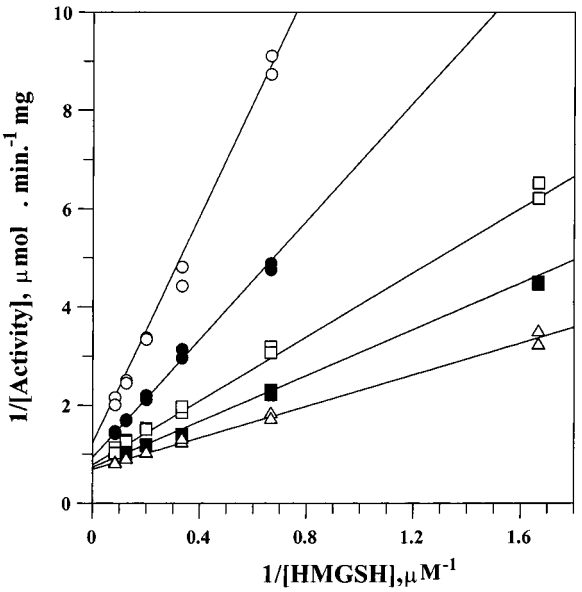

FIGURE 2: Initial velocity patterns for the oxidation of *S*-(hydroxymethyl)glutathione at 25 °C in 0.1 M phosphate buffer (pH 7.5). Double-reciprocal plots showing the rates when the *S*-(hydroxymethyl)glutathione (HMGSH) concentration was varied at various fixed levels of NAD^+: (○) 0.5, (●) 1, (□) 2, (■) 3, and (△) 5 μM NAD^+. The HMGSH concentrations were calculated using eq 2. The lines represent the fits of the data to eq 4. Table 1 shows the values of constants calculated from the fit.

Table 1: Kinetic Constants for the Oxidation of *S*-(Hydroxymethyl)glutathione (HMGSH) and 12-HDDA by Human Glutathione-Dependent Formaldehyde Dehydrogenase[a]

varied substrate (A)	K_a (μM)	K_{ia} (μM)	k_{cat} (min^{-1})
HMGSH	0.80 ± 0.2	18.4 ± 4.0	62.3 ± 3.1
NAD^+	0.47 ± 0.1	11.0 ± 2.9	62.3 ± 3.1
12-HDDA	21 ± 1.7	69.0 ± 8.6	13.0 ± 0.5
NAD^+	5.1 ± 0.4	17.0 ± 2.3	13.0 ± 0.5

[a] Kinetic constants were determined at 25 °C in 0.1 M potassium phosphate buffer (pH 7.5) by varying the concentrations of HMGSH or 12-HDDA and NAD^+ under initial velocity conditions. The data were fit to eq 4, and estimates of the parameters are shown with the associated standard error. K_a and K_{ia} represent the Michaelis−Menten constant and the dissociation constant with HMGSH, 12-HDDA, or NAD^+ as the varied substrate (A). The changing fixed substrate is identified as substrate B in eq 4. A molecular mass of 40 kDa was used to calculate k_{cat} values.

The effect of glutathione on the oxidation of *S*-(hydroxymethyl)glutathione was studied to determine whether it is an allosteric activator as reported previously (*16*). Equation 2 was used to calculate the initial concentrations of glutathione and formaldehyde to obtain concentrations of free glutathione and *S*-(hydroxymethyl)glutathione. Glutathione was not found to have a significant activating or inhibitory effect on *S*-(hydroxymethyl)glutathione oxidation within the 0.1−2 mM range. Moreover, glutathione did not have any significant inhibitory effect on 12-HDDA oxidation at concentrations up to 5 mM.

Product and dead-end inhibition studies were performed to determine whether the kinetic mechanism was ordered or random. 12-ODDA was utilized as the aldehyde product inhibitor in these studies. Studies were carried out by varying the concentrations of one of the substrates [*S*-(hydroxym-

Table 2: Product and Dead-End Inhibition Patterns for the Oxidation of *S*-(Hydroxymethyl)glutathione and 12-HDDA[a]

variable substrate	constant substrate[b]	product inhibitor	type of inhibition[c]	K_{is} (μM)
S-(hydroxymethyl)glutathione	NAD^+ (5)	NADH	C	0.13 ± 0.01
NAD^+	*S*-(hydroxymethyl)glutathione (80)	NADH	C	0.28 ± 0.03
NAD^+	12-HDDA (100)	NADH	C	0.20 ± 0.01
12-HDDA	NAD^+ (12.5)	12-ODDA	C	0.51 ± 0.04
NAD^+	12-HDDA (30)	12-ODDA	C	0.33 ± 0.02

Dead-End Inhibition Patterns Using Dodecanoic Acid as the Inhibitor[a]

variable substrate	constant substrate[b]	type of inhibition[c]	K_{is} (μM)	K_{ii} (μM)
S-(hydroxymethyl)glutathione	NAD^+ (100)	C	23 ± 1.8	–
NAD^+	*S*-(hydroxymethyl)glutathione (1.1)	NC	31 ± 3.4	100 ± 7.9
12-HDDA	NAD^+ (10)	C	33 ± 2.5	–
NAD^+	12-HDDA (60)	NC	51 ± 5.6	122 ± 8.9

[a] Inhibition experiments were performed at 25 °C in 0.1 M potassium phosphate (pH 7.5). During each experiment, a minimum of five concentrations of the varied substrate were used while the concentration of the other substrate was held at a constant value shown in parentheses. A minimum of three inhibitor concentrations were used. The K_{is} and K_{ii} estimates are listed with their associated standard errors. [b] The concentration of the fixed substrate is expressed in micromolar in the parentheses. [c] The data were fit to a competitive, noncompetitive, or uncompetitive model. The type of inhibition shown represents the best fit of the data to the given model as judged from χ^2 analysis. In the case of competitive inhibition, the differences in the χ^2 values obtained from the fits to competitive and noncompetitive models were not significant as judged by the *F* statistics. However, the K_{ii} values obtained from the fit to noncompetitive model were not statistically significant.

ethyl)glutathione, 12-HDDA, or NAD^+] while keeping the other substrate level constant in the absence or presence of different amounts of one of the products (NADH or 12-ODDA). The NAD^+ versus NADH, *S*-(hydroxymethyl)-glutathione versus NADH, and 12-HDDA versus 12-ODDA product inhibition patterns all fit linear competitive inhibition (Table 2). These data are consistent with a random bi-bi mechanism.

The competitive product inhibition pattern of NAD^+ versus 12-ODDA changed to nonintersecting noncompetitive inhibition pattern when the concentration of the fixed substrate 12-HDDA was increased from 30 to 200 μM (Figure 3). The intercept replots were linear, but the slope replots were curved and appeared to be parabolic. This suggests that 12-ODDA was combining with more than one enzyme species.

Additional support for the random mechanism was obtained by examining the dead-end inhibition by dodecanoic acid. Dodecanoic acid was found to be a competitive inhibitor of *S*-(hydroxymethyl)glutathione and 12-HDDA, suggesting that it binds in the alcohol-binding site (Table 2). The double-reciprocal plots for inhibition of NAD^+ by dodecanoic acid at fixed levels of either *S*-(hydroxymethyl)glutathione or 12-HDDA fit noncompetitive inhibition. The experiments suggest that the inhibitor can bind before as well as after the variable substrate NAD^+. Hence, the data are consistent with random addition of substrates to the enzyme during catalysis.

Initial Velocity, Product Inhibition, and Dead-End Inhibition Studies of the Reduction of 12-ODDA. The kinetics of aldehyde reduction were studied using 12-ODDA as the aldehyde substrate. 12-ODDA exhibited partial substrate inhibition at high concentrations (Figure 4A). This substrate inhibition was more pronounced at lower NADH concentrations (not shown). Higher NADH concentrations not only decreased the extent of substrate inhibition by 12-ODDA but also delayed the onset of its substrate inhibition. An apparent K_m of 17 μM for 12-ODDA was calculated using noninhibitory substrate concentrations. The double-reciprocal plots of the initial velocities against varying NADH concentrations at different fixed levels of 12-ODDA (varying from noninhibitory levels to inhibitory levels) were linear, and each fit the Michaelis−Menten equation (Figure 4B).

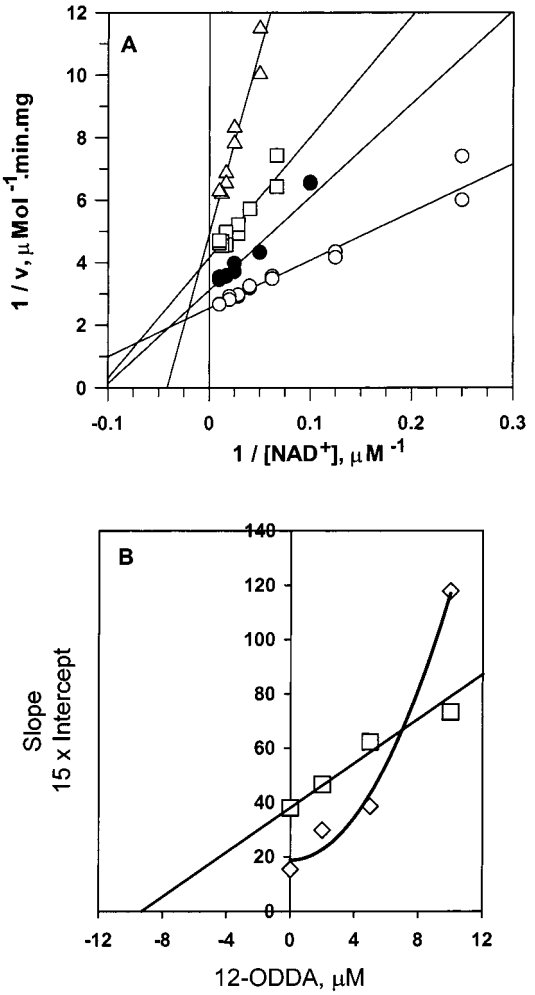

FIGURE 3: Inhibition of glutathione-dependent formaldehyde dehydrogenase by 12-ODDA as the product inhibitor. (A) Double-reciprocal plots showing rates when the NAD^+ concentration was varied in the presence of 200 μM 12-HDDA and (○) 0, (●) 2, (□) 5, and (△) 10 μM 12-ODDA. Individual curves show the fit of each data set to eq 3. (B) The slopes (◇) and intercepts (□) determined in panel A are plotted against the 12-ODDA.

The pattern formed by the double-reciprocal plots with NADH as the variable substrate (Figure 4B) is described as

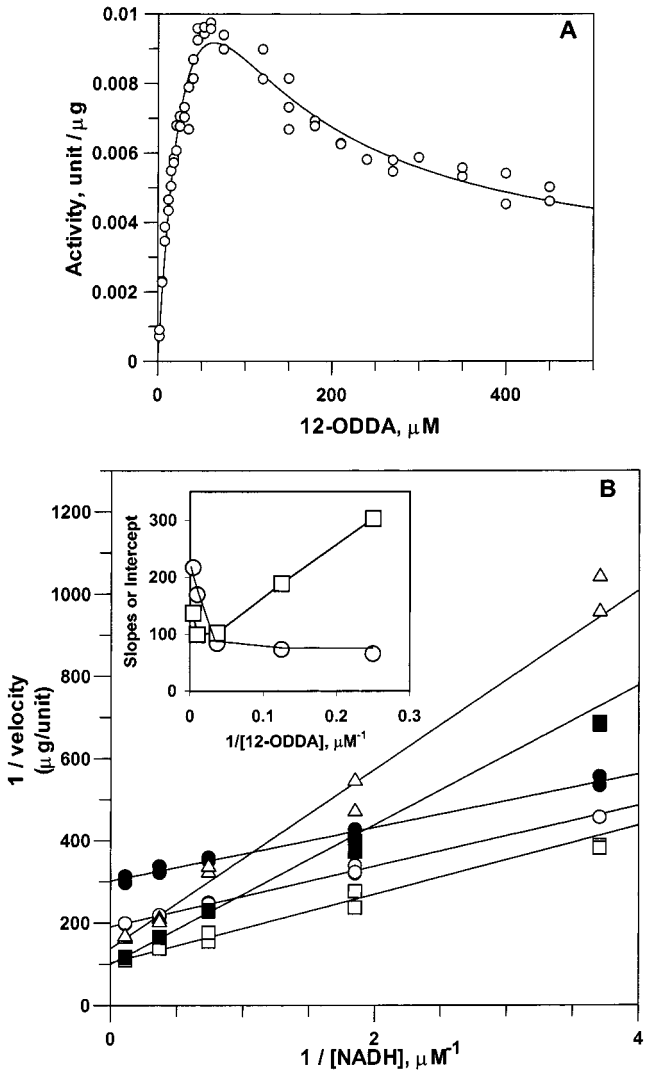

FIGURE 4: (A) Dependence of the glutathione-dependent formaldehyde dehydrogenase-catalyzed reaction rate on 12-ODDA concentrations. The rate of 12-ODDA reduction was determined in the presence of 50 μM NADH at 25 °C in 0.1 M potassium phosphate (pH 7.5). Using nonlinear regression, the data were fit to the steady-state random equation $v = i[A]^2 + j[A]/k + l[A]^2 + m[A]$ described by Ferdinand (*28*), where [A] is the concentration of 12-ODDA and $i-m$ are constants with no apparent physiological significance. The constants were found to have the following values: $i = (7.2 \pm 3.0) \times 10^{-7}$; $j = 4.4 \times 10^{-4} \pm 3.3 \times 10^{-5}$; $k = 1.2$; $l = 3.8 \times 10^{-4} \pm 6.0 \times 10^{-5}$; $m = 1.9 \times 10^{-2} \pm 5.2 \times 10^{-3}$. The fit of the data to the steady-state random equation was found to be significant on the basis of F statistics. (B) Double-reciprocal plots showing rates when the NADH concentration was varied at various fixed levels of 12-ODDA: (●) 4, (○) 8, (□) 27, (■) 100, and (△) 220 μM 12-ODDA. Fitting the individual data set to eq 3 generated the lines. The slopes (○) and intercepts (□) were determined from the fit of each data set in panel A to eq 3 and are plotted against 1/[12-ODDA] in the inset.

noncompetitive substrate inhibition (*23*), in which both the slope and intercept replots against 1/[12-ODDA] are hyperbolic (Figure 4B inset).

Product and dead-end inhibition studies for the aldehyde reduction were performed to determine whether the substrates were adding randomly or in an ordered manner during catalysis. These studies involved adding one of the products of the reverse reaction (12-HDDA or NAD^+) as an inhibitor while varying one of the substrates at fixed levels of another. 12-ODDA was limited to concentrations not showing substrate inhibition. The interpretation of the product inhibition results of the aldehyde reduction was complex because NAD^+ was a competitive inhibitor of NADH at fixed concentrations of 12-ODDA, whereas 12-HDDA was a noncompetitive inhibitor of 12-ODDA reduction (Table 3). The double-reciprocal plot of NAD^+ inhibition against 12-ODDA yielded lines that curved upward as they approached the $1/v$ axis. The linear part of the plots best fit the uncompetitive inhibition equation (eq 7) (Table 3). These results are consistent with an ordered mechanism with NADH binding first to the enzyme during aldehyde reduction or a random mechanism with a preferred pathway and/or dead-end complexes.

The kinetic mechanism of the aldehyde reduction was further investigated using dead-end inhibitor 12-aminododecanoic acid (12-ADDA). During the search for substrate analogs, 12-ADDA was found to be a competitive inhibitor of both 12-ODDA and octanal. It was a noncompetitive inhibitor of 12-HDDA and octanol, suggesting that it formed the E·12-ADDA and E·NADH·12-ADDA dead-end complexes. 12-ADDA was a noncompetitive inhibitor with respect to NADH at constant levels of 12-ODDA (Table 3). Thus, 12-ADDA could bind before NADH as well as after it, further supporting a random mechanism for the reverse reaction.

Equilibrium Binding Studies. Equilibrium binding studies were performed to determine whether both FDH·coenzyme and FDH·alcohol complexes are formed as predicted by the random bi-bi kinetic mechanism. Quenching of native enzyme fluorescence and resonance energy transfer was used to assess the formation of binary complexes. NAD^+ caused a 25% reduction in intrinsic tryptophan enzyme fluorescence, indicating formation of the E·NAD^+ complex. Binding studies with 12-HDDA could not be performed because there was no significant fluorescence change observed. 12-ODDA caused a 5−10% decrease in enzyme fluorescence, evidence of the formation of the E·12-ODDA complex. Resonance energy transfer from tryptophan to NADH was used to monitor the binding of NADH to the free enzyme (Figure 5). The dissociation constant K_d of NAD^+ was found to be 11.5 μM (Table 4), which was in agreement with its K_{ia} value of 11 μM (Table 1). The dissociation constants of NADH and 12-ODDA of 43 and 110 nM, respectively, were lower than but in general agreement with their K_{is} values (Table 2) corrected for the concentration of the nonvaried substrate. 12-HDDA increased the level of resonance energy transfer from the tryptophan in FDH to NADH bound in the active site. This suggested that an E·NADH·12-HDDA abortive complex is formed. The dissociation constant of 12-HDDA for dissociation from the E·NADH·12-HDDA complex was found to be 170 μM.

DISCUSSION

We undertook the kinetic study of glutathione-dependent formaldehyde dehydrogenase in an attempt to clarify discrepancies in reports of its kinetic mechanism (*10*, *15*, *16*). Formaldehyde and glutathione combine in a nonenzymatic reaction to form *S*-(hydroxymethyl)glutathione, which is oxidized by this NAD^+-dependent dehydrogenase. The pH dependence of the reactivity of nucleophilic groups in glutathione is an important factor that determines which

Table 3: Product and Dead-End Inhibition Patterns for the Reduction of 12-ODDA[a]

variable substrate	constant substrate[b]	product inhibitor	type of inhibition[c]	K_{is} (μM)	K_{ii} (μM)
NADH	12-ODDA (20)	NAD^+	C	6.5 ± 0.41	−
12-ODDA	NADH (5)	NAD^+	UC or NC[d]	−	32 ± 2.5
12-ODDA	NADH (5)	12-HDDA	NC	245 ± 30	233 ± 40

Dead-End Inhibition Patterns Using 12-ADDA as the Inhibitor[a]

variable substrate	constant substrate[b]	type of inhibition[c]	K_{is} (μM)	K_{ii} (μM)
12-ODDA	NADH (5)	C	165 ± 7.6	−
NADH	12-ODDA (30)	NC	191 ± 28	401 ± 23

[a] Inhibition experiments were performed at 25 °C in 0.1 M potassium phosphate (pH 7.5). During each experiment, a minimum of five concentrations of the varied substrate were used while the concentration of the other substrate was held at a constant value shown in parentheses. A minimum of three inhibitor concentrations was used. The K_{is} and K_{ii} estimates are listed with their associated standard errors. [b] The concentration of the fixed substrate is expressed in micromolar in parentheses. [c] The data were fit to a competitive, noncompetitive, or uncompetitive model. The type of inhibition represents the best fit of the data to the given model as judged from the χ^2 analysis. In the case of competitive inhibition, the differences in the χ^2 values obtained from the fits to competitive and noncompetitive models were not significant as judged by the F statistics. However, the K_{ii} values obtained from the fit to noncompetitive model were statistically insignificant. [d] The double-reciprocal plot curved as it approached the $1/v$ axis. The linear portion of the curve fitted the uncompetitive model better than the other models.

adducts are formed. The ionization states of sulfydryl and amino groups in glutathione direct the reaction of formaldehyde to form *S*-(hydroxymethyl)glutathione or N-alkylated derivatives. Our ^{13}C NMR experiments indicate that *S*-(hydroxymethyl)glutathione is the only adduct formed when the glutathione concentration exceeds the formaldehyde concentration at pH 7.5, suggesting that part of the disparity between reports may result from the formation of nonoxidizable adducts (Figure 1A, **II** and **III**) when the concentration of formaldehyde exceeded that of glutathione. The circulating levels of glutathione and formaldehyde in vivo are about 5 and 0.1 mM, respectively (*24*). Hence, unless much higher concentrations of formaldehyde are encountered, *S*-(hydroxymethyl)glutathione will be the predominant adduct formed in vivo.

The initial studies of the kinetic mechanism for formaldehyde dehydrogenase, using either *S*-(hydroxymethyl)-glutathione or octanol as the substrate, suggested either ordered or random bi-bi mechanisms (*10*, *15*, *16*). In some cases, initial rate kinetics did not fit simple Michaelis−Menten relationships and glutathione was suggested to be an allosteric regulator (*16*). In our experiments, all the substrates except 12-ODDA fit simple Michaelis−Menten saturation kinetics. We found that the kinetics of the oxidative reaction using *S*-(hydroxymethyl)glutathione or 12-HDDA as a substrate are consistent with a random bi-bi mechanism that is in rapid equilibrium. The experiments for reduction of 12-ODDA are consistent with a steady-state random mechanism. 12-ODDA showed substrate inhibition, which is consistent with the presence of a preferred pathway for substrate addition in the reductive reaction and formation of an abortive E·NAD^+·12-ODDA complex.

Random addition of substrates to FDH in both the oxidative and reductive reactions (Scheme 1) is supported by equilibrium binding, steady-state kinetic, and inhibition studies. Equilibrium binding studies enabled detection of three of the four possible binary complexes in the proposed random bi-bi mechanism (Table 4). The competitive inhibition patterns for the oxidative reaction (Table 2) show that both substrates in both directions bind to the free enzyme. Dead-end inhibition studies with dodecanoic acid and 12-ADDA show that 12-HDDA and 12-ODDA bind before as well as after NAD^+ and NADH, respectively. Competitive and noncompetitive inhibition of 12-ADDA against 12-

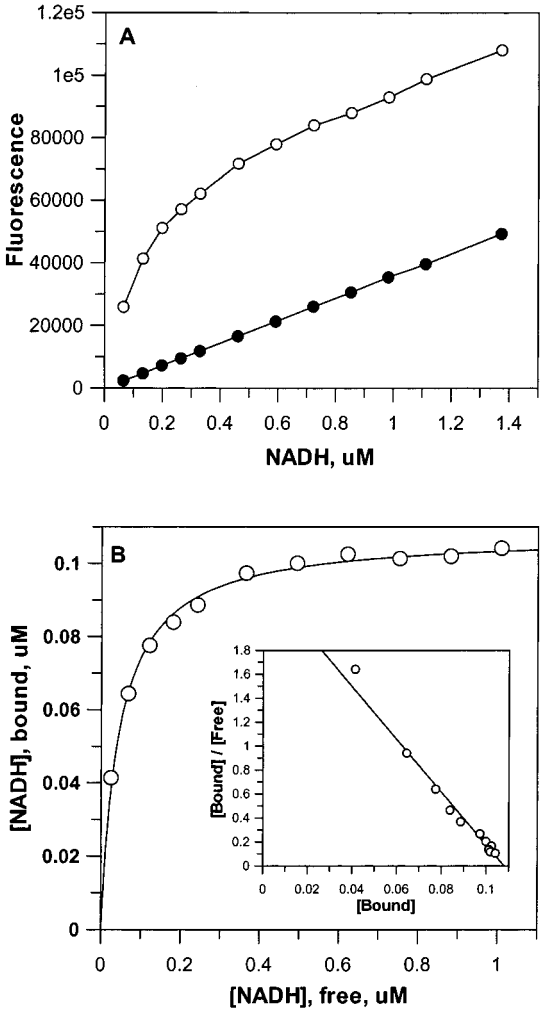

FIGURE 5: Binding of NADH to glutathione-dependent formaldehyde dehydrogenase. The binding of NADH to FDH was monitored by following the resonance energy transfer where the emission from the tryptophans in the protein (excited at 290 nm) was absorbed by the NADH, which reemitted the light at 460 nm. (A) The fluorescence at 460 nm with addition of NADH to 0.105 μM enzyme (○) or buffer (●) is plotted. The excitation wavelength was 290 nm. The studies were conducted in 3 mL of 50 mM phosphate buffer (pH 7.5) at 25 °C. (B) Scatchard analysis of the data performed by nonlinear regression using Grafit 4.0.10. The K_d was estimated in this experiment to be 0.0453 ± 0.002 μM with a capacity of 1.02 binding sites per monomer.

Table 4: Dissociation Constants for the Formation of Indicated Enzyme Complexes As Determined by Fluorescence Spectroscopy[a]

enzyme complex	K_d (μM)	enzyme complex	K_d (μM)
E·NAD$^+$	11.5 ± 2.7	E·12-ODDA	0.11 ± 0.05
E·NADH	0.043 ± 0.01	E·NADH·12-HDDA	170 ± 0.01

[a] Equilibrium binding studies were conducted at 25 °C in 50 mM potassium phosphate buffer (pH 7.5). The data were analyzed by a Scatchard plot, and the estimates of the constants are shown with the associated standard deviation. In the case of the E·NADH·12-HDDA complex, the K_d of 12-HDDA for the E·NADH complex was calculated.

Scheme 1

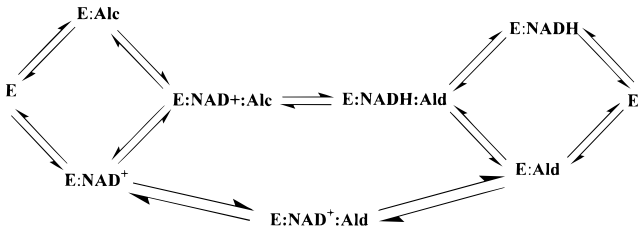

ODDA and 12-HDDA, respectively, are consistent with the ability of 12-ADDA to bind the free enzyme. The noncompetitive substrate inhibition by 12-ODDA is also consistent with a random mechanism.

For random mechanisms exhibiting linear double-reciprocal plots, the addition of substrates may be in rapid equilibrium or at steady state with an equal rate through either of the binary enzyme·substrate complexes. The linear double-reciprocal plots (Figure 2) and competitive product inhibition patterns (Table 2) for the oxidative reaction are more consistent with the rapid equilibrium mechanism where the rate-determining step is after ternary complex formation. For bovine liver formaldehyde dehydrogenase, the rate-determining step for the forward reaction was suggested to be one of the product release steps, since no kinetic isotope effect was observed for *S*-(hydroxymethyl)glutathione oxidation (*25*).

Formation of E·NADH·alcohol and E·NAD$^+$·aldehyde abortive complexes in the catalytic pathway has been described for various alcohol dehydrogenase isozymes (*26*, *27*). Equilibrium binding studies yielded evidence for formation of an E·NADH·12-HDDA abortive complex in FDH, although it was not detected by steady-state kinetic methods. The dissociation constant of 12-HDDA for the E·NADH complex was only 3-fold higher than its K_{ia} value determined kinetically and about 8-fold higher than its Michaelis−Menten constant (Tables 1 and 4). Despite the reasonably high affinity for the E·NADH complex, 12-HDDA showed no substrate inhibition up to concentrations of 1 mM at saturating and unsaturating fixed levels of NAD$^+$ (data not shown). This suggests that the E·NADH·12-HDDA abortive complex is not kinetically significant under steady-state conditions.

Even though the formation of an E·NAD$^+$·12-ODDA complex could not be detected by fluorescence binding methods, the product inhibition by 12-ODDA versus NAD$^+$ (Figure 3) and substrate inhibition during the reductive reaction (Figure 4) could be consistent with its formation. The 12-ODDA versus NAD$^+$ product inhibition pattern changed from competitive to nonlinear noncompetitive as the concentration of the constant substrate, 12-HDDA, was changed from 30 to 200 μM (Table 2 and Figure 3). This could be explained by the fact that at 30 μM 12-HDDA the inhibition by 12-ODDA was resulting from formation of the E·12-ODDA complex and at 200 μM 12-HDDA the inhibition was resulting from the formation of both E·12-ODDA and E·NAD$^+$·12-ODDA complexes. Raising the concentration of 12-HDDA from 30 to 200 μM increased the apparent inhibition constant of 12-ODDA for the free enzyme to a level close enough to that for it to form the E·NAD$^+$·12-ODDA complex. Thus, formation of E·12-ODDA resulted in the slope effect, while formation of the E·NAD$^+$·12-ODDA complex resulted in both slope and intercept effects (Figure 3B).

Substrate inhibition by 12-ODDA was noncompetitive since both the slope and intercept replots were hyperbolic (Figure 4B inset). The most likely explanation for this substrate inhibition is the presence of a preferred pathway in the random mechanism and the formation of the E·NAD$^+$·12-ODDA abortive complex during the reduction of 12-ODDA for the following reasons. (a) The addition of substrates during the reduction of 12-ODDA is random. This was evident from equilibrium binding studies, noncompetitive substrate inhibition studies, and dead-end and product inhibition studies in Tables 2 and 3. (b) The slope effects (Figure 4B inset) with substrate inhibition by 12-ODDA cannot result from the formation of the E·NAD$^+$·12-ODDA abortive complex alone. (c) Formation of an E·NAD$^+$·12-ODDA abortive complex was evident from 12-ODDA versus NAD$^+$ product inhibition experiments and could also give rise to substrate inhibition. (d) Nonhyperbolic initial velocities of the kind observed with 12-ODDA (in Figure 4A and replot of the data in Figure 4B as velocity vs [12-ODDA]) are expected in a random bi-bi system where one of the alternate pathways is kinetically favored over another (*28*). Hence, we suggest that the rate is slower through the E·12-ODDA complex. The addition of substrates during the reduction of 12-ODDA should be in the steady state because substrate inhibition is not possible in a rapid equilibrium random mechanism unless one of the substrate binds abortively in the active site of the other one. Overall, the kinetic data are consistent with the random bi-bi kinetic mechanism shown in Scheme 1.

The three-dimensional structure of human glutathione-dependent formaldehyde dehydrogenase (class III alcohol dehydrogenase) revealed unique features relative to published class I alcohol dehydrogenase structures that are consistent with the kinetic mechanism and substrate specificity reported here. Class I alcohol dehydrogenases show a substantial conformational change upon binding of NAD$^+$ or NADH (*29*, *30*). These dimeric enzymes have a coenzyme domain that forms the subunit interface and a catalytic domain located away from the interface. The active site is situated in the cleft between catalytic and coenzyme domains. The catalytic domain rotates by about 10° following coenzyme binding and limits coenzyme release from the active site in the closed conformation (*31*). The extent of the domain movement is similar in the binary and ternary complexes. The domain movement and the binding of the coenzyme are necessary for formation of the alcohol-binding site (*31*−*34*) and the alignment of critical catalytic residues. Hence, the coenzyme-induced conformational change is consistent with the ordered bi-bi kinetic mechanism of class I alcohol dehydrogenases with coenzyme binding to the free enzyme.

The structure of the binary complex of formaldehyde dehydrogenase with NAD^+ [1TEH (*35*)] exhibits structural features that are consistent with a random kinetic mechanism. In this structure, the orientation of the catalytic domain relative to the coenzyme domain is halfway between that observed in the class I apo structure and the binary and/or ternary structures. This has been called the semi-open domain structure (*35*, *36*). The NAD^+ binding site in this semi-open conformation is solvent-exposed, making coenzyme dissociation possible without any domain movement. Furthermore, substrates *S*-(hydroxymethyl)glutathione and 10-hydroxydecanoate were easily modeled into the substrate-binding site without any domain change in the semi-open conformation (*35*). Both NAD^+ and *S*-(hydroxymethyl)-glutathione can readily diffuse from this ternary complex in any order. The random bi-bi mechanism deduced from the kinetic and equilibrium binding studies is consistent with this semi-open domain structure (*35*).

A random mechanism dictates that the apoenzyme be able to bind the alcohol or aldehyde substrate in the absence of the coenzyme and vice versa. Apoenzyme may have a semi-open structure similar to that observed for the formaldehyde dehydrogenase·NAD^+ binary complex structure (*35*). This may allow the apoenzyme to bind the alcohol (or aldehyde) substrate in the absence of the coenzyme. There may be a further closing of the structure in the productive ternary complex to align the catalytic residues optimally for catalysis.

ACKNOWLEDGMENT

We thank Dr. Alan M. Mahrenholz for his help in the electrospray ionization mass spectrometry of 12-oxododecanoic acid and Ms. Julia Walker for performing preliminary kinetic studies. The NMR spectroscopy in this paper was performed at the NMR center of the IUPUI Department of Physics.

REFERENCES

1. Duester, G., Farres, J., Felder, M. R., Holmes, R. S., Hoog, J.-O., Pares, X., Plapp, B. V., Yin, S.-J., and Jornvall, H. (1999) *Biochem. Pharmacol. 58*, 389−395.
2. Harris, D. K. (1953) *Br. J. Ind. Med. 10*, 255−268.
3. Romaguera, C., Grimalt, F., and Lecha, M. L. (1981) *Contact Dermatol. 7*, 152−153.
4. Morgan, K. T., Jiang, X. Z., Starr, T. B., and Kerns, W. D. (1986) *Toxicol. Appl. Pharmacol. 82*, 264−271.
5. International Agency for Research on Cancer (1995) *Wood Dust and Formaldehyde*, IARC Monographs on the Evaluation of Carcinogenic Risks to Humans 62, pp 217−362, International Agency for Research on Cancer, Lyon, France.
6. Mashford, P. M., and Jones, A. R. (1982) *Xenobiotica 12*, 119−124.
7. Uotila, L., and Koivusalo, M. (1989) in *Coenzymes and cofactors, glutathione. Chemical, biochemical and medical aspects* (Dolphin, D., Poulson, R., and Avramovic, O., Eds.) pp 517−551, John Wiley and Sons, New York.
8. Koivusalo, M., Baumann, M., and Uotila, L. (1989) *FEBS Lett. 257*, 105−109.
9. Wagner, F. W., Pares, X., Holmquist, B., and Vallee, B. L. (1984) *Biochemistry 23*, 2193−2199.
10. Julia, P., Boleda, M. D., Farres, J., and Pares, X. (1987) *Alcohol Alcohol.* (Suppl. 1), 169−173.
11. Kaiser, R., Holmquist, B., Vallee, B. L., and Jornvall, H. (1989) *Biochemistry 28*, 8432−8438.
12. Shafqat, J., El-Ahmad, M., Danielsson, O., Martinez, M. C., Persson, B., Pares, X., and Jornvall, H. (1996) *Proc. Natl. Acad. Sci. U.S.A. 93*, 5595−5599.
13. Danielsson, O., and Jornvall, H. (1992) *Proc. Natl. Acad. Sci. U.S.A. 89*, 9247−9251.
14. Iborra, F. J., Renau-Piqueras, J., Portoles, M., Boleda, M. D., Guerri, C., and Pares, X. (1992) *J. Histochem. Cytochem. 40*, 1865−1878.
15. Uotila, L., and Mannervik, B. (1980) *Biochim. Biophys. Acta 616*, 153−157.
16. Uotila, L., and Mannervik, B. (1979) *Biochem. J. 177*, 869−878.
17. Giri, P. R., Krug, J. F., Kozak, C., Moretti, T., O'Brien, S. J., Seuanez, H. N., and Goldman, D. (1989) *Biochem. Biophys. Res. Commun. 164*, 453−460.
18. Sharma, C. P., Fox, E. A., Holmquist, B., Jornvall, H., and Vallee, B. L. (1989) *Biochem. Biophys. Res. Commun. 164*, 631−637.
19. Hurley, T. D., Edenberg, H. J., and Bosron, W. F. (1990) *J. Biol. Chem. 265*, 16366−16372.
20. Corey, E. J., and Schmidt, G. (1979) *Tetrahedron Lett. 5*, 399−402.
21. Bryant, F., and Overell, B. T. (1953) *Biochim. Biophys. Acta 10*, 471−476.
22. Naylor, S., Mason, R. P., Sanders, J. K., Williams, D. H., and Moneti, G. (1988) *Biochem. J. 249*, 573−579.
23. Cleland, W. W. (1970) in *The Enzymes* (Boyer, P. D., Ed.) pp 1−65, Academic Press, San Diego.
24. Heck, H., Casanova-Schmitz, M., Dodd, P. B., Schachter, E. N., Witek, T. J., and Tosun, T. (1985) *Am. Ind. Hyg. Assoc. J. 46*, 1−3.
25. Pourmotabbed, T., Shih, M. J., and Creighton, D. J. (1989) *J. Biol. Chem. 264*, 17384−17388.
26. Shearer, G. L., Kim, K., Lee, K. M., Wang, C. K., and Plapp, B. V. (1993) *Biochemistry 32*, 11186−11194.
27. Hanes, C. S., Bronskill, P. M., Gurr, P. A., and Wong, J. T. (1972) *Can. J. Biochem. 50*, 1385−1413.
28. Ferdinand, W. (1966) *Biochem. J. 98*, 278−283.
29. Eklund, H., Samma, J. P., Wallen, L., Branden, C. I., Akeson, A., and Jones, T. A. (1981) *J. Mol. Biol. 146*, 561−587.
30. Al-karadaghi, S., Cedergren-Zeppezauer, E., Petrantos, K., Hovmoller, S., Terry, H., Dauter, Z., and Wilson, K. S. (1994) *Acta Crystallogr. D50*, 793−807.
31. Ramaswamy, S., Eklund, H., and Plapp, B. V. (1994) *Biochemistry 33*, 5230−5237.
32. Eklund, H., Muller-Wille, P., Horjales, E., Futer, O., Holmquist, B., Vallee, B. L., Hoog, J. O., Kaiser, R., and Jornvall, H. (1990) *Eur. J. Biochem. 193*, 303−310.
33. Eklund, H., Plapp, B. V., Samama, J. P., and Branden, C. I. (1982) *J. Biol. Chem. 257*, 14349−14358.
34. Eklund, H., and Branden, C. I. (1979) *J. Biol. Chem. 254*, 3458−3461.
35. Yang, Z. Y., Bosron, W. F., and Hurley, T. D. (1997) *J. Mol. Biol. 265*, 330−343.
36. Ramaswamy, S., El-Ahmad, M., Danielsson, O., Jornvall, H., and Eklund, H. (1996) *Protein Sci. 5*, 663−671.

BI9929711